

1
2
3
4
5
6
7
8
9
10
11
12
13
14
15
16
17
18
19
20
21

Determination of optimum vibro-compaction time using sound analysis

Bazoumana Sanogo¹, Duygu Kocaefe^{1*}, Yasar Kocaefe¹, Dipankar Bhattacharyay¹², Jules Côté³

¹ UQAC Research Chair on Industrial Materials (CHIMI), University of Quebec at Chicoutimi,
555, Boulevard de l'Université, Chicoutimi, QC, Canada G7H 2B1

² Presently working at Centurion University of Technology and Management, Odisha, India
752050

³ Aluminerie Alouette, 400, chemin de la Pointe-Noire, C.P. 1650
Sept-Îles, QC, Canada G4R 5M9

Bazoumana Sanogo¹, (bazoumana.sanogo1@uqac.ca)

Duygu Kocaefe^{1*}, (Duygu_Kocaefe@uqac.ca),

Yasar Kocaefe¹, (Yasar_Kocaefe@uqac.ca)

Dipankar Bhattacharyay¹², (dipankar.bhattacharyay@cutm.ac.in)

Jules Côté³, (jcote@alouette.qc.ca)

Corresponding author: Duygu_Kocaefe@uqac.ca

Tel: 418-545-5011 / 5215

22 **Abstract**

23 The quality of carbon anodes plays an essential role in the production of primary aluminum. The
24 vibro-compaction is one of the most important steps of the anode fabrication process, which affects
25 the anode quality. Over and under-compacting results in anodes with high electrical resistivity,
26 poor mechanical and physical properties. Therefore, the compaction conditions should be chosen
27 carefully. A method and a sound analysis software were developed to determine the optimum
28 vibration time using the sound generated by the vibro-compactor during anode compaction. This
29 method was tested with a bench-scale system both in the laboratory and in the plant. It is simple,
30 fast and inexpensive. The effect of anode raw materials (types of coke and pitch) and top-former
31 bellows pressure of the vibro-compactor on the optimum compaction time as well as the effect of
32 compaction time on anode properties were investigated. The results showed that there are three
33 stages of anode formation during vibro-compaction, good quality anodes can be produced by using
34 compaction time around the optimal value, and the utilization of sound analysis reduces the
35 compaction time.

36 **Keywords:** Carbon anodes, vibro-compaction, optimum compaction time, aluminum production,
37 under-compaction, over-compaction

38 **1. Introduction**

39 Primary aluminum is produced by electrolysis via Hall-Héroult process [1, 2] using carbon anodes,
40 graphite cathodes, and alumina dissolved in cryolite. The energy required for the reduction of
41 alumina to aluminum is supplied by electrical energy. The carbon anodes are produced using
42 calcined petroleum coke, rejected green and baked anodes, recycled butts (aggregate) and coal tar
43 pitch (binder). The anode paste obtained by mixing all the raw materials is compacted in a vibro-
44 compactor to produce green anodes. The green anodes baked in open-pit anode baking furnaces to
45 produce the baked anodes [3-4]. Then, the baked anodes are cooled and rodded before sending
46 them to electrolysis. The baking step sets the final properties of the anodes. Defects (cracks, pores)
47 formed during baking might be result of baking conditions as well as the raw material quality, and
48 the green anode production conditions such as the parameters of mixing, compaction, and cooling.

49 The quality of anodes is very important in the production process, because it affects the metal
50 quality, the production costs, and the greenhouse gas emissions. Furthermore, bad quality anodes
51 disturb the stability of the electrolysis process and may cause the cell to dysfunction [5, 6]. Thus,
52 the improvement of anode quality has become a concern for aluminum industry. The industry is
53 constantly looking for better solutions through the implementation of quality control tools with the
54 objective of approaching the optimum operation parameters of each unit involved in anode
55 production.

56 Vibro-compactor has different operational parameters such as vibration force, frequency, and the
57 compaction time, which affect the anode properties [7, 8]. The compaction time is one of the key
58 parameters which is easy to adjust during the operation. An improper compaction time results in
59 under-compacted or over-compacted green anodes, and reduces the anode quality. Hulse [9] found
60 that the under-compacted anodes have larger porosity which results in reduced density and
61 mechanical properties, and increased electrical resistivity. Porous anodes also lead to higher
62 carbon consumption (operational cost) due to increased rates of side reactions with air and CO₂
63 (anode reactivity), consequently, higher GHG emissions. Furthermore, the energy consumption
64 (operational cost) increases due to higher electrical resistivity. Over-compaction create stresses in
65 the green anode, which causes crack formation during baking, again increasing the anode electrical
66 resistivity [10]. Both under-compaction and over-compaction decrease the yield of the alumina
67 reduction (aluminum production). There are a few studies on the impact of compaction time on

68 anodes throughout the literature. Hulse [9] has shown that the physical, mechanical, and electrical
69 properties of the green anodes improve with increasing compaction time and pitch rate until the
70 optimal compaction time is reached. Then, they start to deteriorate. Tkac [11] also obtained similar
71 results.

72 There are also some attempts reported in the literature for determining the optimum compaction
73 time of green anodes. Gao et al. [12] developed a method for determining the optimal compaction
74 time by following the movement of a bar attached to the compactor cover. The time when the
75 movement of the bar stopped was defined as the optimal compaction time. They correlated the
76 optimal time with the anode size. According to this study, anode with a given size had one optimum
77 compaction time. They did not consider that the anodes with similar sizes can have different
78 optimum compaction times due to the non-homogeneity of raw materials, thus the anode paste.
79 Jonathan et al. [10] used the acceleration of the vibro-compactor table to optimize the anode
80 formation and correlated the green anode density with the compaction time, but the determination
81 of optimum compaction time was difficult with this method.

82 During the present study, a method, a bench scale equipment, and a sound analysis software were
83 developed to determine the suitable compaction time for each individual anode by using the sound
84 generated by the vibro-compactor during the green anode formation. The sound was recorded via
85 a microphone and analyzed with the developed software. In general, the compaction time is kept
86 constant in the plants. However, due to the non-homogeneity of the raw materials, the optimum
87 compaction time may be different for each anode. This method was validated and tested both on
88 laboratory and industrial anodes.

89 Audible sound between 16 Hz to 16 kHz [13] was also used in different areas such as machine
90 tools and machining [14], diesel engines [15], gears [16], welding [17], biology [18], and road
91 safety [19]. An application of sound in primary aluminum production was also reported in the
92 literature. It was applied to electrolysis cells as non-destructive methods to prevent anomalies
93 during cell operation (both Söderberg and prebaked). The quality of the anodes was correlated
94 with the sound of the bubbles recorded in the cell [20-21]. They found that the high gas flow
95 through the anode cracks reduces the bubble noise underneath the anode. Therefore, low noise
96 points out to the high number of cracks. Also, other problems such as the presence of anode pieces
97 that has to be removed from the pot, splashing, erosion of gas manifolds, bath level, spike setting,

98 etc. can be related to sound produced by gas bubbles in the cell. The present study is the first study
99 which uses the sound analysis to determine the optimum compaction time, thus improve green
100 anode quality.

101 **2. Methodology**

102 A bench-scale experimental system was set up and a sound analysis software was developed to
103 determine the optimum compaction time for each anode. The method was based on the change in
104 the sound emitted by the vibro-compactor during the formation of green anodes.

105 The experiments were carried out both in the laboratory and in the plant. The laboratory scale
106 anodes were produced in the carbon laboratory of the UQAC Research Chair on Industrial
107 Materials/Chaire institutionnelle sur les matériaux industriels (CHIMI). The industrial anodes
108 were produced in Aluminerie Alouette Inc. Sept-Îles plant.

109 **2.1. Sound analysis**

110 The software uses the "Fast Fourier Transform" (FFT), which is a method generally used for
111 acoustics measurements. FFT converts the discrete data into a continuous data at different
112 frequencies. The sound was recorded in time domain and converted to frequency domain. Thus, at
113 any point of time, there was a value of sound intensity corresponding to each frequency. As, due
114 to noises or other reasons, the intensity of sound for adjacent frequencies may vary and the
115 variation would be difficult to analyze, averages for intensities corresponding to n number of
116 frequencies were determined. That average intensity corresponding to the average of the
117 frequencies was utilized for analysis. The averaging reduced spikes and helped in determining the
118 change in sound level. A code in visual basic was developed for this purpose.

119 After the sound is recorded, the data is smoothed by taking the average of each (n) points. Then,
120 the appropriate analysis frequency range (F) was determined. These two parameters play an
121 essential role in signal processing. Subsequently, visualization of the results facilitates the
122 determination of the optimal time sought. The recording and analysis of sound can be done
123 simultaneously or sequentially.

124 The number of points (n) is used to smooth the sound curve in order to highlight irregularities in
125 the signals as well as to eliminate undesired noise. This facilitates the determination of the phases
126 of compaction and of the optimum compaction time. Thus, the value of (n) is determined by

127 keeping all the parameters constant and changing only (n). If (n) is too high, data is smoothed too
128 much resulting in the loss of the characteristics of the curve. If it is too low, it is hard to detect the
129 characteristics of the curve due to existing noise.

130 While a part of the recorded sound comes from the vibro-compactor, there are sounds coming from
131 other equipment around the vibro-compactor. In order to eliminate this secondary noise and
132 facilitate the comparison of the results, it is necessary to choose the suitable frequency range (F).
133 The sound is therefore viewed as a function of time but in a frequency range. In order to determine
134 the (F), the other parameters are fixed while the frequency range is varied. The desired range must
135 have a fast (instantaneous) response and must clearly describe the phases of compaction.

136 Once determined, same (F) and (n) are used to analyze all the sound data. At the end, the data is
137 converted back to the time domain with the Inverse Fourier Transformation (IFT). Using the rate
138 of change in sound level and the defined thresholds, the different phases and the optimal time of
139 compaction are determined.

140 **2.2. Bench-scale equipment**

141 **2.2.1. Bench-scale experimental system**

142 The experimental systems used in the laboratory and the plant are presented in Figure 1. It is
143 composed of a unidirectional microphone placed next to the vibro-compactor and a data
144 acquisition system which includes the developed sound analysis software. Unidirectional
145 microphone captures the sounds in a specific direction from a space in a shape of cardioid. It
146 eliminates the sounds in all other directions.

147

148

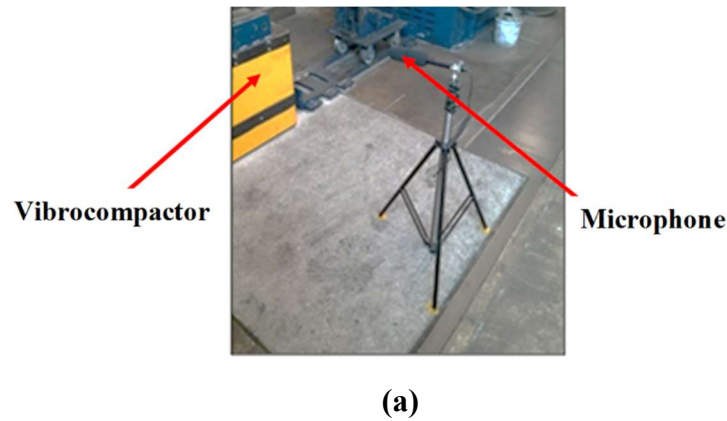
149

150

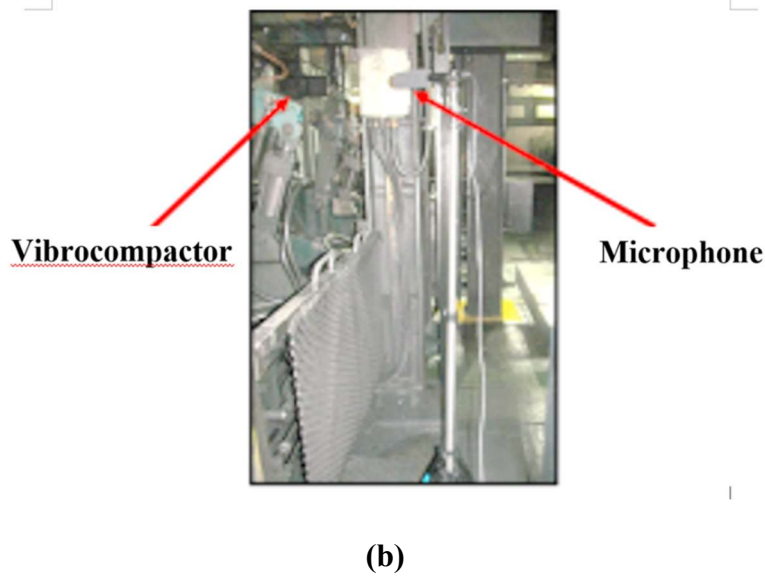
151

152

153



154



155

156 Figure 1: Bench-scale experimental system used in (a) the laboratory and (b) the plant

157 **2.2.2. Experimental study in the laboratory**

158 To produce the laboratory anodes, first calcined coke, rejected anodes, and butts (part of the anodes
159 recuperated after the electrolysis) with a certain particle size distribution are mixed with pitch
160 (binder) in an intensive mixer. This anode paste is compacted in a vibro-compactor to form a green
161 anode. The sound of the vibro-compactor is registered for each anode.

162 The quality of the anodes depends on the raw materials (type of coke, the type of pitch, the particle
163 size), the operating parameters used during anode production. These parameters affect the anode
164 properties; therefore, they influence the optimal compaction time.

165 Two series of tests were carried out in the laboratory. The anodes produced in the carbon laboratory
166 of Chair CHIMI at UQAC have similar properties to those of industrial anodes. Therefore, the

167 validation of the method was carried out with the laboratory anodes. In the first series, four anodes
168 (Anode L1 to Anode L4) were produced using the compaction times $t_1 > t_4 > t_2 > t_3$ for the
169 validation. (L) indicates the laboratory anodes. t_4 was the standard compaction time. Therefore,
170 the anode produced using this time was taken as the standard (reference) anode. t_2 was the
171 optimum compaction determined with the sound analysis. The anode produced by compacting the
172 anode t_2 s and stopping the compaction manually when this time was detected by the software.

173 In the second series, two groups of anodes were made. First, four anodes (Anode L5 to Anode L8)
174 were produced using the compaction time of the standard anode (t_4) and baked using different
175 heating rates. It is important to note that the same standard heating rate (h) was used up to 600°C ,
176 then the different heating rates were applied. The most of the volatiles are released before this
177 temperature. Therefore, relatively slower heating rate (h) was used below 600°C in order to avoid
178 a rapid volatile release which can cause crack formation. Above 600°C , heating rates faster than
179 the standard ($h_1 < h_2 < h_3 < h_4$) were used in order to compensate for the time lost due to the
180 utilization of low heating rate below 600°C , hence increase the anode production rate.

181 After, another six anodes (Anode L9 to Anode L14) were produced with the aim of studying the
182 effects of raw materials (types of pitch and coke) on compaction time.

183 The anodes were characterized by measuring their density, resistivity and compressive strength
184 according to ASTM D5502-00, ASTM D6120-97, and ASTM C695-91:2005 [22, 23, 24],
185 respectively. These properties were correlated with the compaction time to determine if the anodes
186 are under or over-compacted.

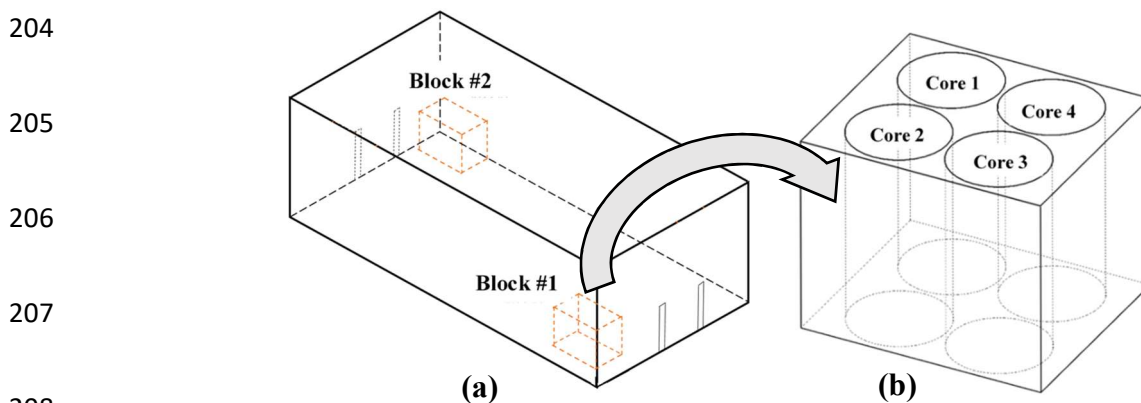
187 **2.2.3. Industrial measurement campaign**

188 The plant tests were carried out during the industrial measurement campaign. First, the software
189 was improved and the experimental system was standardized by determining the best position of
190 the equipment relative to the vibro-compactor and the parameters in order to capture the vibro-
191 compactor sound, and the first tests were carried out.

192 Then, the tests were carried out at the plant to study the effect of pitch percentages (Anode I1, to
193 Anode I3), and variation of the top-former bellow pressure of the compactor (Anode I4 and Anode
194 I5). The vibrating table represents one of the most important elements constituting a vibro-
195 compactor. This table is isolated by using air cushions made of inflatable rubber. The top-former

196 bellow pressure refers to the pressure of the top air cushion. In order to obtain anodes which are
197 produced using the optimum compaction time, the compaction was manually stopped when the
198 optimum compaction time was detected by the software similar to the laboratory experiments.

199 These anodes were characterized in the carbon laboratory of Chair CHIMI at UQAC by measuring
200 their density, electrical resistivity and compressive strength according to ASTM standards
201 mentioned in the previous section. The characterization was carried out with 60 cores extracted
202 from the industrial anodes. To do this, two small blocks were removed from the anodes (Figure
203 2(a)). These blocks were then cored as shown in Figure 2(b).



209 Figure 2: (a) Extraction and (b) coring plan of small anode blocks

210 After each core was numbered in the form AX-B-C where A is the anode number (Anode I1 to
211 Anode I5 where (I) indicates the industrial anodes), B is the block number, and C is the core
212 number. For example, A1-1-3 indicates that the core 3 comes from the block 1 of anode number
213 1.

214 3. Results and discussion

215 The results are presented in dimensionless form due to the confidentiality of the industrial results.
216 They are obtained by dividing the values of the parameters by a reference value.

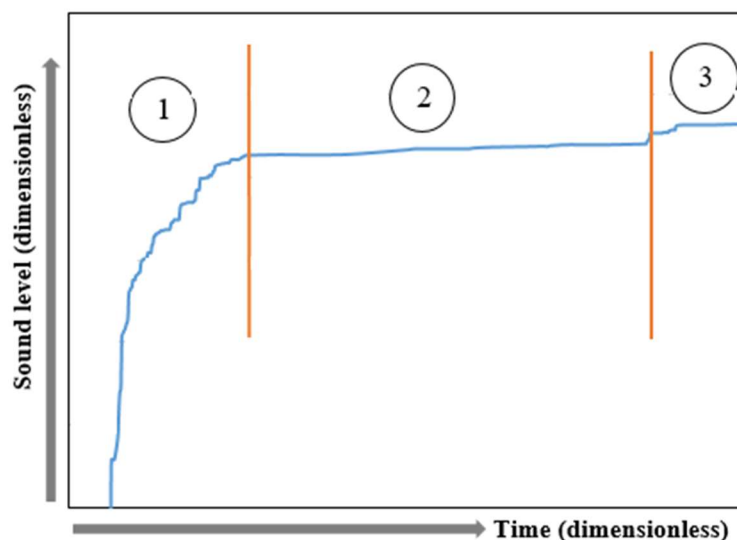
217 3.2. Characterization of the vibro-compaction of anodes

218 The analysis of the sound recorded both in the laboratory and the plant showed that there are three
219 phases of anode compaction as shown in Figure 3:

- 220 • Phase 1: The reorganization of the pitch and coke particles observed as a rapid increase in
221 sound level.
- 222 • Phase 2: The vibro-compaction of anode. In this phase, anode paste is compacted and a
223 green anode is formed. This phase is characterized by a monotonic and flat curve.
- 224 • Phase 3: This phase indicates the end of the compaction. At this stage, the block is
225 sufficiently compact and solid. This phase is observed first as an increase followed by a
226 stabilization of the sound level which indicates the optimum compaction time.

227 Similar trend was observed by Rebaine [8] during the anode paste rigidity measurements in the
228 laboratory.

229



230 Figure 3: The phases of anode vibro-compaction (the optimum compaction time is at the
231 beginning of the last plateau)

232 3.3. Laboratory anodes: Validation of the method

233 As it was explained in the methodology section, three series of anodes were produced in the
234 laboratory.

235 3.3.2. First series of anodes

236 In the first series, four anodes (Anode L1 to Anode L4) were produced at different compaction
237 times ($t_1 > t_4 > t_2 > t_3$), and characterized. t_4 and t_2 are the standard and optimum compaction times,
238 respectively. These results were used to validate the method developed.

239 During characterization, green anode density (GAD), baked anode density (BAD), baked anode
240 resistivity (BAR) and mass loss during anode baking were measured. The optimum time was
241 detected for each anode during vibro-compaction using sound analysis. The over-compaction time
242 was calculated by determining the difference between the actual compaction time used during the
243 anode production and the optimum compaction time found from the sound analysis. Table 1
244 presents the results. In order to show the impact of compaction time on anode density, the over-
245 compaction time is correlated with the BAD/GAD ratio (Figure 4). As it can be seen from this
246 figure, the BAD/GAD ratio is greatest for the anode manufactured at the optimum compaction
247 time (Anode L2 at t2) for which the residual stress due to the compaction is low in the anode.
248 Utilization of this time prevents significantly the formation of cracks during the volatile release.
249 This means that the anodes compacted with the compaction times of t1 (Anode L1) and t4 (Anode
250 L4) are over-compacted whereas the anode compacted with the compaction time of t3 (Anode 3)
251 are under-compacted.

252 The mass loss during anode baking is presented in Figure 5, and GAD and BAR are presented in
253 Figure 6. The results for the mass loss are similar, and the anode with the optimum compaction
254 time (Anode 2, L2, t2) has the second lowest mass loss. The electrical resistivity results show a
255 similar trend, BAR of the anode with the optimum compaction time (Anode 2, L2, t2) has the
256 second lowest value. Anode 1 (L1, t1) has the highest green density since it was the most over-
257 compacted anode with longest compaction time. This anode (Anode 1, L1, t1) has also the highest
258 mass loss and the lowest BAD/GAD ratio. Anode 3 (under-compacted) and Anode 4 (over-
259 compacted) had higher electrical resistivities compared to that of Anode 2, which is compacted
260 using the optimum time. The under-compacted anode (Anode 3) is indicated with a negative over-
261 compaction time. Although it is over-compacted, the resistivity of Anode L1 is slightly lower than
262 that of Anode L2. This is probably due to the higher green density of this anode compared to that
263 of Anode L2.

264

265

266

267

268

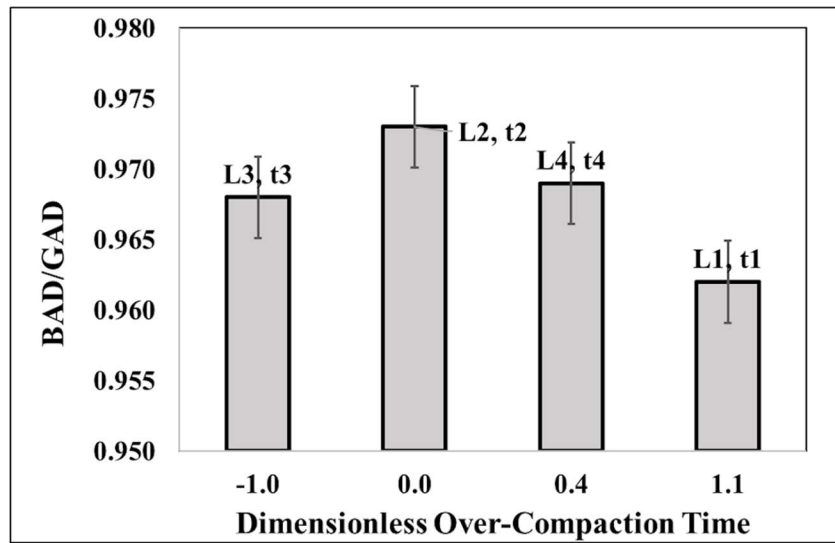
Table 1: Results of the first validation (values are dimensionless)

Anode	Compaction time	Optimum compaction time	Over-compaction time	GAD	BAD	BAD/GAD	BAR	Mass loss (%)
L1	t ₁	0.678	1.122	1.087	1.046	0.962	0.970	4.25
L2	t ₂	0.660	0	1.060	1.031	0.973	1.041	4.11
L3	t ₃	-	- 0.990	1.030	0.997	0.968	1.230	4.15
L4	t ₄	0.764	0.436	1.037	1.005	0.969	1.145	4.07

269

270

271

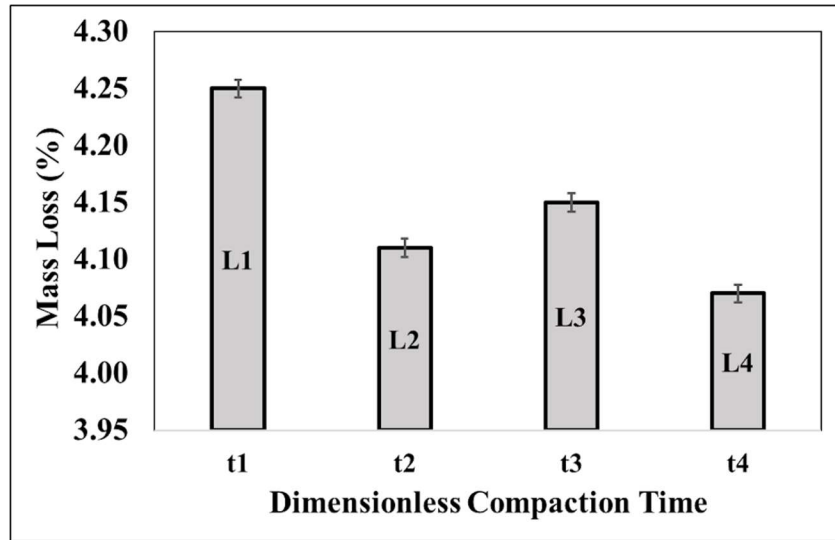


272

273

Figure 4: BAD /GAD of anodes as a function of over-compaction time

274

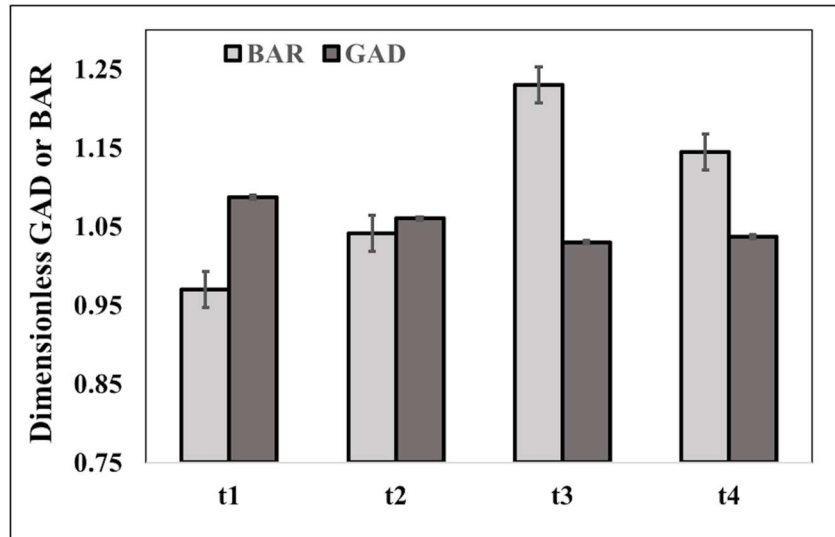


275

276

277

Figure 5: Mass loss during baking



278

279 Figure 6: The electrical resistivity of the baked anodes and the density of the green anodes

280

281 3.3.3. Second series of anodes

282 For the second series, another four anodes (Anode L5 to Anode L8) were produced using the

283 standard compaction time and their over-compaction time was calculated by taking the difference

284 between the compaction time used and the optimum time determined with the sound analysis. They

285 were baked with the heating rate of “h” up to 600°C and with higher heating rates
286 (h<h1<h2<h3<h4) afterwards. The results are presented in Table 2.

287 Although the same compaction time was used for these anodes, each has a different over-
288 compaction time. This is due to the non-homogeneity of the raw materials used, which is the case
289 also in the plant. This shows that the determination the compaction time of each individual anode
290 will help to improve their quality.

291 Anode L7 had a compaction time close to the optimum time whereas Anode L5 was the most over-
292 compacted anode. Anodes L6 and L8 were also over-compacted with similar over-compaction
293 times. Figure 7 shows that the Anode L7 had the highest and Anode L5 has the lowest BAD/GAD
294 ratio. Anodes L6 and L8 had similar over-compaction times, thus their BAD/GAD ratios were also
295 similar.

296 As it can be seen from Table 2 and Figure 7, the BAD/GAD ratio is dependent on the over-
297 compaction time, and increasing the heating rate after most of the volatiles are released, did not
298 affect the results. This shows that the heating rate can be increased after 600°C to increase the
299 production rate without affecting the anode quality.

300

301

Table 2: Results of the second validation (values are dimensionless)

Anode	Heating* rate	Optimum compaction time	Over- compaction time	Green anode density (GAD)	Baked anode density (BAD)	BAD/GAD
L5	h, h1	0.764	0.436	1.096	1.061	0.969
L6	h, h2	0.851	0.349	1.099	1.069	0.972
L7	h, h3	1.171	0.029	1.089	1.061	0.974
L8	h, h4	0.878	0.322	1.089	1.059	0.972

302

h<h1<h2<h3<h4

303

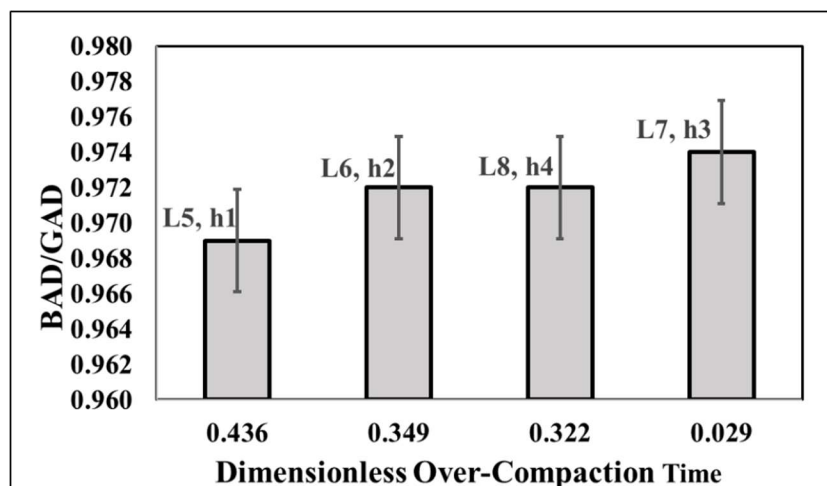


Figure 7: BAD/GAD vs, over-compaction time for the second series of anodes

3.2.3 Third series of anodes

3.2.3.1 Pitch type

Three anodes (Anode L9 to Anode L11) were produced using three different pitches. All the anodes were manufactured under standard conditions with the exception of the type of pitch. The three types of pitch used had different percentages of quinoline insolubles ($QI1 < QI3 < QI2$). Also, the size of the QI particles was different ($p_{QI1} < p_{QI2} < p_{QI3}$). Anode L9 was produced with the pitch (P1) containing smallest size QI (QI1) particles whereas the size of QI particles (QI3) was largest in the pitch (P3) used for the production of Anode L11. The anodes were baked and characterized. It can be seen from

Figure 8 presents GAD and BAD/GAD as a function of over-compaction time. GAD of the anode (L11) produced with the largest QI particles is the smallest, and GAD of the one produced with the smallest QI particles is the highest (L9). This result is in agreement with the previous work [25]. It was found that the pitch with greater QI particle size penetrates less into the pores of the coke particles, thus leading to a lower density since the pitch did not fill all the particle pores.

It can also be seen from the same figure that BAD/GAD increases with decreasing over-compaction time. BAD/GAD is largest for the anode (L11) which has the lowest over-compaction time probably due to less crack formation. The over-compacted anodes have usually more pores and cracks forming due to the release of the stresses created during vibro-compaction and the release of volatiles at the different stages of baking [9].

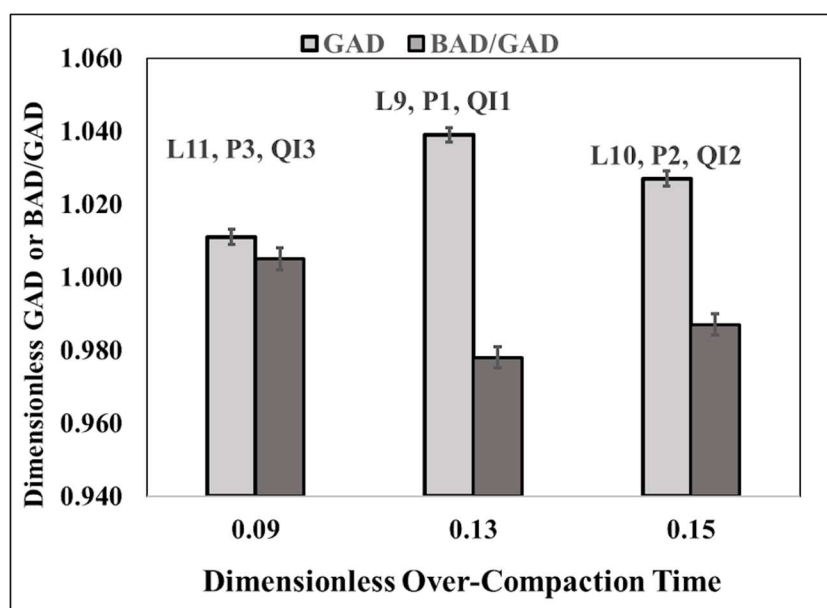
326

Table 3: Results for the anodes produced with different pitches

Anode	Pitch/ QI content/ QI particle size (p_{QI})	Optimum compaction time	Over- compaction time	GAD	BAD	BAD/GAD
L9	P1 / QI1 % / Smallest	1.070	0.130	1.039	1.015	0.978
L10	P2 / QI2 % / Medium	1.050	0.150	1.027	1.014	0.987
L11	P3 / QI3 % / Largest	1.110	0.090	1.011	1.017	1.005

327 $QI1 < QI3 < QI2$; $p_{QI1} < p_{QI2} < p_{QI3}$

328



329

330 Figure 8: GAD and BAD/GAD as a function of compaction time of anodes made with pitches
 331 containing different QI content ($QI1 < QI3 < QI2$) and QI particle size ($p_{QI1} < p_{QI2} < p_{QI3}$)

332 3.2.3.2. Coke type

333 Three anodes were produced with three different types of coke (Anode L12 to Anode L14). These
 334 cokes represent a mixture of two types of coke: low sulfur coke (LSC) and high sulfur coke (HSC).
 335 Thus, their sulfur contents were different. Coke (Coke 1, S1) used for Anode L12 had the lowest
 336 sulfur content whereas coke (Coke 3, S3) used for Anode L14 had the highest. All the anodes were
 337 produced under the same standard conditions. Only the type of coke was different.

338 The results show that the GAD increases with increasing sulfur content as can be seen in Figure 9
 339 and Table 4. Previous work has shown that low-sulfur coke has a higher percentage of open pores
 340 than high sulfur coke [26]. Also, it is reported in the literature that the increasing sulfur content
 341 increases the wettability of coke by pitch [27]. Therefore, Anode L12 has the lowest GAD and
 342 Anode L14 has the highest GAD.

343 Again, the anode with the lowest over-compaction time (Anode L12) gives the highest BAD/GAD
 344 value. Anodes L13 and L14, which have relatively close over-compaction times (Table 4), have
 345 similar BAD/GAD values. This means that a compaction time that is closer to the optimum time
 346 result in less crack formation better BAD/GAD.

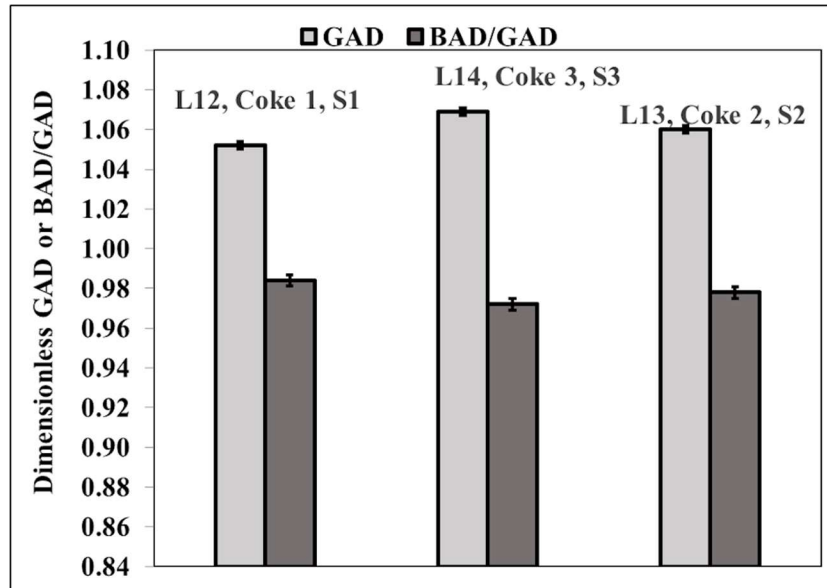
347 The results obtained from the laboratory anodes validate the developed method showing that the
 348 anodes compacted using the optimum time, in general, have better BAD/GAD ratios. This means
 349 if the compaction is stopped at the right moment, the anode does not build up extra stress that is
 350 released during baking leading to crack formation. The raw materials (pitch and coke) used in the
 351 plants are mixture of the raw materials coming from different suppliers. The composition of each
 352 anode can be slightly different. The results show the importance of determining the optimum
 353 compaction time for each anode. Even the anodes produced under similar conditions might have
 354 different optimum compaction times due to the non-homogeneity of the raw materials.

355 Table 4: Results for the anodes produced with different cokes (values are dimensionless)

Anode	% S in coke	Optimum compaction time	Over-compaction time	GAD	BAD	BAD/GAD
L12	S1 (Coke 1)	0.860	0.340	1.052	1.035	0.984
L13	S2 (Coke 2)	0.553	0.647	1.060	1.037	0.978
L14	S3 (Coke 3)	0.664	0.536	1.069	1.039	0.972

356 S1(Coke 1) < S2 (Coke 2) < S3 (Coke 3)

357



358

359 Figure 9: GAD and BAD/GAD as a function of over-compaction time of anodes made with
 360 cokes containing different sulfur contents ($S1 < S2 < S3$)

361

362 3.3. Plant measurement campaign results

363 In the plant, there are different noises. The noises may arise from different parts of the vibro-
 364 compactor or other equipment. The objective was to record the sound of the cover of the compactor
 365 mold hitting the anode top surface. Thus, distance and position of the microphone with respect to
 366 the vibro-compactor mold was adjusted so that there was minimum noise captured from other
 367 equipment and reasonable sound of the cover was captured. Maximizing the sound from the mold
 368 was not the only criteria, minimization of other noises was also necessary. The level of sound
 369 generated from the mold was less of a concern. The ability to record changes in sound level due to
 370 the impact of mold cover with the anode surface was important. Based on this understanding, the
 371 position of the microphone was determined. The position of the microphone was maintained the
 372 same for all the measurements. The position may vary for other plants or other vibro-compactors.

373 First, the equipment is calibrated by determining the position of the microphone (ATR6550 used
 374 at the normal mode) and its distance from the industrial vibro-compactor. After, the effects of the
 375 pitch percentage and top-former bellow pressure were studied.

376

377

378 **3.3.1. Pitch percentage**

379 Three industrial anodes were produced to study the effect of the pitch percentage on compaction
 380 time in the plant (Anode I1, to Anode I3) containing different percentages of the same pitch (Table
 381 5). Anode I3 had the lowest and Anode I2 had the highest pitch percentages (PP3<PP1<PP2).
 382 Anode I2 had the highest density since it had the highest pitch percentage and the lowest over-
 383 over-compaction time (Table 5). In fact, Anode I1 and Anode I2 have similar BAD/GAD ratios since
 384 they have similar over-compaction times compared to that of Anode I3 (Table 5). These anodes
 385 were produced at compaction times, which are relatively closer to their optimum values, thus
 386 avoiding excess crack formation during baking.

387 Figures 10 shows the electrical resistivity of these anodes before and after baking. It can be noted
 388 that the electrical resistivity decreases with the increase in the pitch percentage as it is also
 389 reported in the literature [9]. Also, the optimum compaction time increases with increasing pitch
 390 percentage (Table 5). Thus, it takes longer to compact an anode as the pitch percentage increases.

391 An addition, pitch helps to fill the void between the particles and in the pores, thus reducing the
 392 electrical resistivity of both green and baked anodes. However, there is a limit for increasing the
 393 pitch percentage. The excess pitch increases the electrical resistivity since electrical resistivity of
 394 pitch is higher than that of the coke but lower than that of the air in the voids. Anode I1 and I2
 395 have similar resistivities in green state showing that this pitch percentage is close to the
 396 maximum.

397

398 Table 5: Densities of the industrial anodes containing different pitch percentages
 399 (PP3<PP1<PP2)

Anode	Pitch %	Over-compaction time	GAD	BAD	BAD/GAD
I1	PP1	0.058	1.112	1.073	0.965
I2	PP2	0.038	1.120	1.079	0.964
I3	PP3	0.183	1.113	1.068	0.959

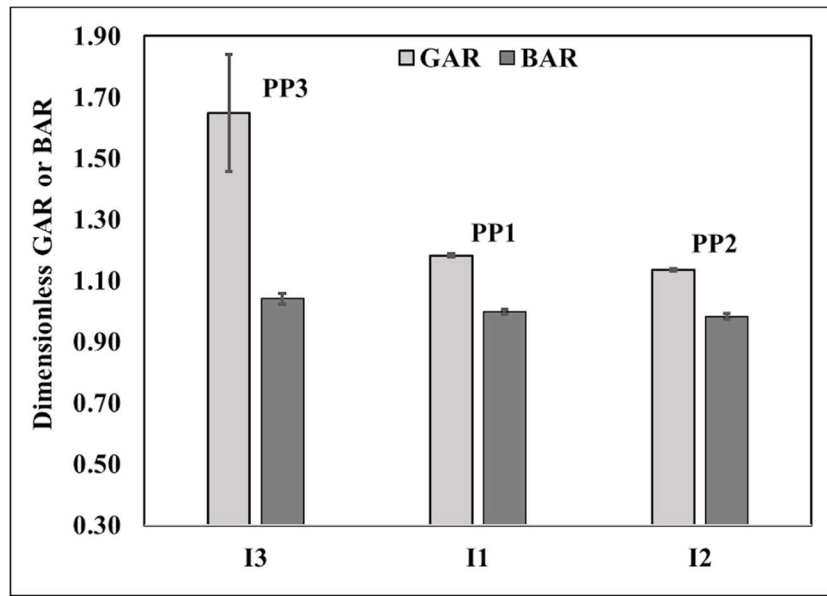
403

404 Table 6: Electrical resistivity and compressive strength of the industrial anodes containing
 405 different pitch percentages (PP3<PP1<PP2)

Anode	Pitch %	Electrical resistivity	
		GAR	BAR
I1	1.010 (P1%)	1.182	0.998
I2	1.020 (P2%)	1.136	0.983
I3	1.000 (P3%)	1.648	1.041

406 GAR: Green anode resistivity; BAR: Baked anode resistivity

407



408

409 Figure 10: Green (GAR) and baked anode (BAR) electrical resistivities (PP3<PP1<PP2)

410

411 **3.3.2. Top-former bellow pressure**

412 The vibrating table of a vibro-compactor is isolated using inflatable rubber cushions (bellows)
 413 filled with compressed air. The pressure of these bellows affects the compression. To evaluate the
 414 impact of the top-former bellow pressure on the compaction time and anode properties, two anodes
 415 (Anode I4 and Anode I5) were produced. Varying this parameter significantly affects the vibro-
 416 compactor performance and can cause problems by exposing the compactor to extreme conditions.

417 Therefore, the range of this parameter is limited. The results shown in Tables 7 and 8 indicate that
 418 the density increased whereas resistivity and optimum compaction time decreased both for green
 419 and baked anodes with increasing top-former bellow pressure. High pressure facilitates the
 420 penetration of pitch between the coke particles and into the coke pores, hence improves the anode
 421 properties within the range studied. This result was also reported in the literature for laboratory
 422 green anodes [8]. It is therefore important to have optimal top-former bellow pressure in order to
 423 have better compaction at an optimum time.

424 Table 7: Optimum compaction time of the anodes produced with different top-former bellow
 425 pressure

Anode	Top-former bellow pressure	Optimum compaction time
I4	1.0	>1
I5	1.2	1

428 Tableau 8: Density, electrical resistivity and compressive strength of the anodes produced with
 429 different top-former bellow pressure

Anode	Density		Electrical resistivity	
	GAD	BAD	GAR	BAR
I4	1.021	0.984	1.906	1.121
I5	1.048	1.011	1.052	1.015

433 4. Conclusions and recommendations

434 The anode quality control is of great importance to the primary aluminum industry. It highly
 435 depends on the operating parameters. An improper choice of compaction time can lead to poor
 436 quality anodes, which cause problems during electrolysis. This article presents a method of
 437 determining the optimum compaction time using the sound of the vibro-compactor recorded during
 438 the compaction. This method makes it possible to determine the optimal compaction time for each
 439 individual anode, consequently leads to the improvement of baked anode properties.

440 Utilization of this method showed that the anodes go through three phases during vibro-
441 compaction. The impact of compaction time on anode properties was assessed. The results showed
442 that anodes compacted at the optimum time or close to the optimum time (low over-compaction
443 time) generally acquire a better baked anode density for a given green anode density (high
444 BAD/GAD ratio).

445 The raw materials affect the green anode density. Higher sulfur-containing coke and pitch with
446 smaller QI particles result in greater green anode density. In any case, the best BAD/GAD ratio is
447 achieved when the compaction time is closer to the optimum value. That is, potentially the best
448 baked anode density for a given green anode density is obtained when the compaction is carried
449 out at the optimum time.

450 **ACKNOWLEDGEMENTS**

451 The technical and financial support of Aluminerie Alouette Inc. as well as the financial support
452 of the Natural Sciences and Engineering Research Council of Canada (NSERC), Développement
453 économique Sept-Îles (DESI), the University of Québec at Chicoutimi (UQAC), and the
454 Foundation of the University of Québec at Chicoutimi (FUQAC) is greatly appreciated (Grant
455 number: CRDPJ 451986 - 13).

456 **REFERENCES**

- 457 [1] Ivan G, Plateau J. Le brevet de Paul Héroult pour un procédé électrolytique de préparation
458 d'aluminium, Bibnum [En ligne], Sciences de l'ingénieur, 2009; <http://bibnum.revues.org/66>.
459 [accessed 6 April 2021]
- 460 [2] Charette A, Kocaefe YS, Kocaefe D. Le carbone dans l'industrie de l'aluminium. Chicoutimi
461 (Québec): Les presses de l'aluminium (PRAL); 2012.
- 462 [3] Severo DS, Gusberti V, Pinto EC. Advanced 3D modelling for anode baking furnaces. Light
463 Metals 2005; 697-702. http://www.caetebr.com/download/CT_Severo.pdf
- 464 [4] Baiteche M, Kocaefe D, Kocaefe Y, Marceau D, Morais B. Description and applications
465 of a 3D mathematical model for horizontal anode baking furnaces. Light Metals 2015; 1115-
466 20. <https://constellation.uqac.ca/5026/>
- 467 [5] Vlasov A, Sizyakov V, Seregin, D, Molin M, Idiyatulin R. Reducing the incidence of anode
468 effects at the Krasnoyarsk aluminum plant, Metallurgist 2011; 55(7): 601-6.

- 469 https://www.researchgate.net/publication/257622228_Reducing_the_incidence_of_anode_eff
470 [ects_at_the_Krasnoyarsk_aluminum_plant](https://www.researchgate.net/publication/257622228_Reducing_the_incidence_of_anode_eff)
- 471 [6] Ye SL, Xiao J, Ding FQ, Li J, Zou Z, Liu YX. Comprehension properties of carbon anode for
472 aluminum electrolysis. Chinese Journal of Nonferrous Metals 2003; **13**(2): 490-95.
- 473 [7] Paskota M. On modelling and the control of vibroformers in aluminium production. Chaos,
474 Solitons & Fractals 1998; 9(1-2): 323-35.
475 <https://www.sciencedirect.com/science/article/pii/S0960077997000702>
- 476 [8] Rebaïne F. Étude de l'influence des paramètres de vibro-compaction sur les propriétés
477 mécaniques des anodes crues en carbon., Ph.D. Thesis, Université du Québec à Chicoutimi,
478 Québec, Canada 2015. <https://constellation.uqac.ca/3364/>
- 479 [9] Hulse KL. Anode manufacture : Raw materials, formulation and processing parameters. Sierre
480 [Suisse]: R&D Carbon Ltd; 2000.
- 481 [10] Jonathan PH, Arnaud B, Sonia T. Maximising vibroformer performance through
482 vibration monitoring. 10th Australasian Aluminium Smelting Technology Conference;
483 Launceston: Tas.; Australia; 2011.
- 484 [11] Tkac M., Foosnaes T, Øye HA. Effect of vacuum vibroforming on porosity development
485 during anode baking. Light Metals 2007; 885-90.
- 486 [12] Gao S., Bao C, Zhang S, Wang H, Woo J, Cutshall E. Optimum vibration time for green
487 anode production. Light Metals 2013; 1123-26.
- 488 [13] American National Standards Institute (ANSI), ANSI/ASA S1.1-2013, Acoustical
489 Terminology 2013.
- 490 [14] Dornfeld D. Application of acoustic emission techniques in manufacturing. NDT&E
491 International 1992; 25(6): 259-269.
492 <https://www.sciencedirect.com/science/article/pii/096386959290636U>
- 493 [15] Albarbar A, Gu F, Ball, AD. Diesel engine fuel injection monitoring using acoustic
494 measurements and independent component analysis. Measurement 2010; 43(10):1376-86.
495 <https://www.sciencedirect.com/science/article/pii/S0263224110001636>
- 496 [16] Polyshchuk VV. Detection and quantification of the gear tooth damage from the vibration
497 and acoustic signatures. Ph.D. Thesis. The University of Akron, Ann Arbor 1993: 258-258

- 498 [17] Cayo EH, Alfaro, SCA. A Non-Intrusive GMA Welding Process Quality Monitoring
499 System Using Acoustic Sensing. *Sensors* 2009; 9: 7150-66. 7150-7166.
500 <https://doi.org/10.3390/s90907150>
- 501 [18] Kikuchi M, Akamatsu T, Gonzalez-Socoloske D, De Souza DA, Olivera-Gomez LD, Da
502 Silva, VMF. Detection of manatee feeding events by animal-borne underwater sound
503 recorders. *JMBA* 2014; 1139-46.
504 [https://www.researchgate.net/publication/260834815_Detection_of_manatee_feeding_events
505 _by_animal-borne_underwater_sound_recorders](https://www.researchgate.net/publication/260834815_Detection_of_manatee_feeding_events_by_animal-borne_underwater_sound_recorders)
- 506 [19] Saykin VV, Zhang Y, Cao Y, Wang ML, McDaniel, JG. Pavement macrotexture
507 monitoring through sound generated by a tire-pavement interaction. *J. Eng. Mech.* 2013;
508 139(3): 264-71. <https://ascelibrary.org/doi/10.1061/%28ASCE%29EM.1943-7889.0000485>
- 509 [20] Kalgraf K, Jensen M, Pedersen TB. Theory of bubble noise, bath height and anode
510 quality. *Light Metals* 2007; 357-61.
- 511 [21] Marianne J, Tor BP, Kjell K. Bubble noise from soderberg pots. *Light Metals* 2007; 265-
512 68.
- 513 [22] An American National Standard, ASTM D5502-00 (2010), Standard Test Method for
514 Apparent Density by Physical Measurements of Manufactured Anode and Cathode Carbon
515 Used by the Aluminum Industry 2010.
- 516 [23] An American National Standard, ASTM D6120-97 (Reapproved 2007), Standard test
517 method for electrical resistivity of anode and cathode carbon material at room temperature.
518 2010; 1225-27.
- 519 [24] An American National Standard, ASTM C695-91 (Reapproved 2005), Standard test
520 method for compressive strength of carbon and graphite. 2010; 211-13.
- 521 [25] Lu Y, Kocaeffe D, Kocaeffe Y, Bhattacharyay D. Wettability of coke by pitches with
522 different quinolone-insoluble contents. *Fuel* 2017; 199: 587-97.
- 523 [26] Amara, B., Effet du soufre sur la réactivité des anodes en carbone, Master thesis,
524 University of Quebec at Chicoutimi, Québec, Canada 2017.
525 https://constellation.uqac.ca/4230/1/Amara_uqac_0862N_10327.pdf

526 [27] Sarkar A. Effect of coke properties on anode properties. Ph.D. Thesis, University of
527 Quebec at Chicoutimi, Chicoutimi, Quebec, Canada 2015.
528 https://constellation.uqac.ca/3881/1/Sarkar_uqac_0862D_10186.pdf
529